



## Infrasonic jet noise from volcanic eruptions

R. S. Matoza,<sup>1</sup> D. Fee,<sup>2</sup> M. A. Garcés,<sup>2</sup> J. M. Seiner,<sup>3</sup> P. A. Ramón,<sup>4</sup> and M. A. H. Hedlin<sup>1</sup>

Received 1 November 2008; revised 9 February 2009; accepted 20 February 2009; published 18 April 2009.

[1] The lowermost section of a Vulcanian or Plinian volcanic eruption column may be thought of as a momentum-driven, turbulent, free-shear jet flow. We propose that large-amplitude and long-duration infrasonic (<20 Hz) signals recorded at ranges of tens of kilometers during powerful eruptions at Mount St. Helens, USA, and Tungurahua, Ecuador, represent a low frequency form of jet noise. A preliminary test of this hypothesis is made by comparing the observed infrasonic spectra to the empirically-derived similarity spectra for pure-air jets. Although the spectral shapes are in approximate agreement, the observed volcanic signals have additional complexities not present in the pure-air laboratory data. These features may result from multiphase flow containing solid particles and liquid droplets, very high temperatures, and perhaps complex crater morphology. However, the overall similarity between the volcanic signals and jet noise indicates that broadband infrasound measurements at volcanoes may provide a quantitative link to eruption jet dynamics, and would aid substantially in the remote assessment of volcanic hazard. **Citation:** Matoza, R. S., D. Fee, M. A. Garcés, J. M. Seiner, P. A. Ramón, and M. A. H. Hedlin (2009), Infrasonic jet noise from volcanic eruptions, *Geophys. Res. Lett.*, 36, L08303, doi:10.1029/2008GL036486.

### 1. Introduction

[2] Since volcanoes have large length-scales, the majority of their atmospheric acoustic radiation is infrasonic (<20 Hz) [Wilson and Forbes, 1966; Ripepe et al., 1996; Garcés et al., 1998; Vergnolle and Caplan-Auerbach, 2006]. As observed with volcano seismology [Chouet, 1996], a variety of volcanological processes act as sources in this frequency band, each with distinct temporal and spectral characteristics. A continuous vibration of the ground or air is classified as seismic or infrasonic tremor respectively. However, different seismic and infrasonic tremor-generating processes may occur at different volcanoes, and at the same volcano to some degree.

[3] Here we focus on one particular type of infrasonic tremor that was found to accompany powerful Vulcanian and Plinian eruptions at Mount St. Helens (MSH), USA and Tungurahua, Ecuador. The infrasonic tremor signals are of high-amplitude, long-duration, and broadband. If they were to couple into ground vibration and be recorded seismically, they would be classified as eruption tremor [McNutt, 2000].

<sup>1</sup>Laboratory for Atmospheric Acoustics, Institute of Geophysics and Planetary Physics, Scripps Institution of Oceanography, La Jolla, California, USA.

<sup>2</sup>Infrasound Laboratory, University of Hawai'i, Kailua-Kona, Hawaii, USA.

<sup>3</sup>National Center for Physical Acoustics, University of Mississippi, University, Mississippi, USA.

<sup>4</sup>Instituto Geofísico, Escuela Politécnica Nacional, Quito, Ecuador.

However, the data presented here strongly suggest that the source is within the erupted jet in the atmosphere, so is more naturally observed with infrasonic sensors recording atmospheric pressure fluctuations.

[4] Large Vulcanian and Plinian volcanic eruptions may be thought of as turbulent, free-shear jet flows that transition with altitude into buoyancy-driven volcanic plumes [Wilson, 1976; Kieffer and Sturtevant, 1984; Ogden et al., 2008]. Although the acoustic radiation from these fluid dynamic processes remains poorly understood, it has been proposed [Woulff and McGetchin, 1976] that turbulence within small-scale volcanic jets may act as a quadrupole source according to Lighthill's acoustic analogy [Lighthill, 1954], or a dipole source if solid particles or boundaries are present [Woulff and McGetchin, 1976]. However, measurement of the sound radiation pattern from large volcanic eruptions has proven challenging, and poor scaling between acoustic and eruption intensity has been reported [Johnson et al., 2005].

[5] Our data indicate that infrasonic tremor signals recorded at ranges of tens of kilometers during Vulcanian and Plinian eruptions represent a low frequency form of jet noise. Rather than quadrupole radiation from fine-scale turbulence, the signals have spectral properties more characteristic of large-scale turbulence noise. We propose that dynamic similarity in jet flow results in similar physical noise-generation mechanisms in volcanic jets as in audible jet noise from flight vehicles (i.e., jet flow from aircraft and rockets). Since the length-scales for a volcanic jet are much larger, the jet noise is expected at much lower frequencies. Furthermore, we find that as the length-scale and mass flux of the volcanic jet increase, acoustic radiation shifts to lower frequencies with greater power output. This indicates that eruption intensity and acoustic power output scale over a broad acoustic bandwidth.

### 2. Infrasound From Large Eruptions

[6] Figure 1 shows the infrasonic waveforms recorded during a short-lived phreatic eruption (dominantly steam with entrained ash) at MSH on 8 March 2005, and three magmatic eruptions (heavily particle-laden) at Tungurahua that occurred on 14–15 July 2006, 16–17 August 2006, and 6 February 2008. Hereafter, we refer to these eruptions respectively as eruptions A-D (Figure 1). The MSH eruption (A) is best classified as Vulcanian based on its relatively brief duration. The Tungurahua eruptions (B-D) range between Vulcanian, sub-Plinian, and Plinian based on the duration of jetting. The data were recorded on four-element small-aperture arrays of broadband infrasonic sensors deployed at ranges of 13.4 km from MSH [Matoza et al., 2007] and 36.9 km from Tungurahua [Garcés et al., 2008]. The systems deployed at MSH and Tungurahua have a flat response 0.01–17 Hz and 0.1–17 Hz respectively. Array processing [Matoza et al., 2007] confirms the signals as

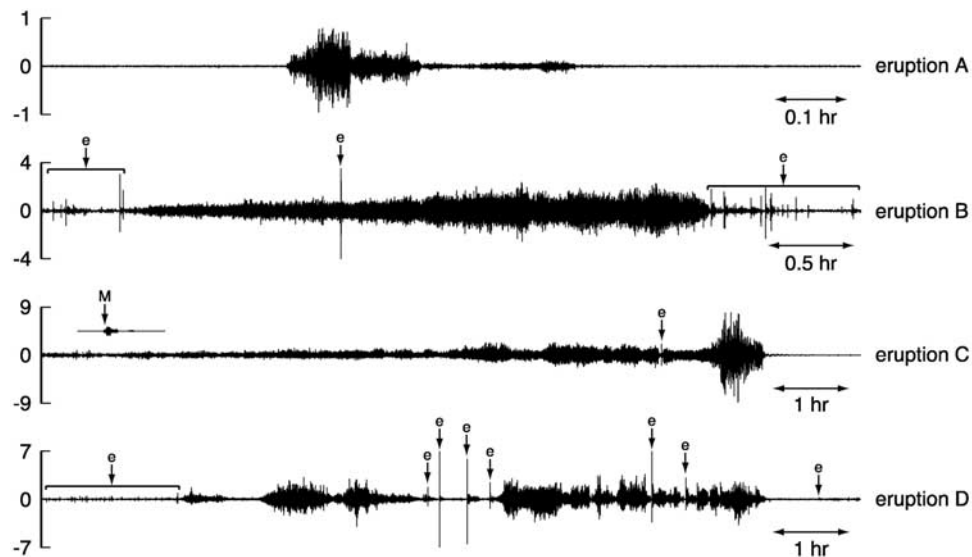


**Figure 1.** Infrasonic signals recorded during Vulcanian-Plinian volcanic eruptions: 8 March 2005 MSH eruption recorded at 13.4 km [Matoza *et al.*, 2007] (eruption A), 14–15 July 2006 (eruption B), 16–17 August 2006 (eruption C), and 6 February 2008 (eruption D) Tungurahua eruptions recorded at 36.9 km. Each trace represents a time-domain beam across four array elements with unit gain. Amplitude scale (left) is in pressure (Pa). Time scale (hours) indicated at lower right of each trace. Discrete explosion occurrences marked by ‘e’. The signal labelled ‘M’ on the third trace is the MSH eruption (eruption A) plot at the same scale for comparison.

coherent acoustic waves arriving from the azimuth of the volcano. Although with different amplitude-scale and duration, each signal in Figure 1 is emergent and broadband, with its amplitude envelope changing over time. Discrete, impulsive explosion signals are recorded at Tungurahua (eruptions B-D) in addition to the emergent broadband signals. Note that the final hour of C is marked by a dramatic increase in signal amplitude with lower dominant frequency, before the tremor ends abruptly. This hour corresponds to a drastic change in the eruptive activity [Barba *et al.*, 2006], characterised by an increase in jet diameter to >400 m, lava fountaining to a height  $\sim 6$  km, and a plume height  $\sim 25$  km (A. Steffke *et al.*, Identifying eruption chronologies, plume heights and eruption styles at Tungurahua volcano: Integrating thermal infrared satellite and infrasound data, manuscript in preparation, 2009).

[7] Despite the apparent complexity of the recorded signals, the dynamic self-similarity of jet flows [Pope, 2005], and the similarity of radiated jet noise spectra [Tam *et al.*, 1996; Tam, 1998] suggest that infrasonic tremor signals from volcanic eruptions and audible jet noise from flight vehicles may be generated by comparable physical mechanisms occurring at different length and time-scales. An illustration of this is achieved by applying time-compression to the digital infrasonic signals (see auxiliary material).<sup>1</sup> After speeding-up the recordings by multiples of a hundred, the signals are audible, and sound qualitatively similar to jet noise from aircraft and rockets.

### 3. Comparison With Jet Noise Spectra

[8] The study of jet noise is intimately related to the study of turbulence, and for this reason a first-principles noise

prediction theory is far from complete [Tam, 1998]. However, it is known that quadrupole radiation attributed to fine-scale turbulence [Lilley, 1991] is just one component of jet noise. Noise attributed to large-scale orderly turbulence structures [Crow and Champagne, 1971], screech, and broadband shock can be important depending on the jet operating conditions [Tam, 1995]. In addition, laboratory studies of pure-air jets have documented precisely the empirical dependence of audible jet noise spectra and radiation patterns on jet operating parameters such as the jet diameter, Mach number, and temperature [Seiner, 1984]. A key discovery has been that jet noise spectra exhibit self-similarity, with the overall shape and curvature of the spectra dependent solely on whether fine-scale or large-scale turbulence is the dominant noise source in a particular direction [Tam *et al.*, 1996]. The frequency band in which jet noise is radiated is related to the expanded jet diameter and velocity via the Strouhal number ( $St = fD_j/U_j$ , where  $f$ ,  $D_j$ , and  $U_j$  are the frequency, expanded jet diameter, and jet velocity respectively) [Seiner, 1984]. For a constant  $St$  and  $U_j$ , a jet with larger  $D_j$  will radiate at lower acoustic frequency  $f$ .

[9] To test whether the self-similarity of jet noise extends to infrasonic eruption tremor signals, we compare the shape of the infrasonic spectra with the similarity spectra [Tam *et al.*, 1996] for audible jet noise. Figure 2 shows power spectral density (PSD) estimates of the signals shown in Figure 1. Since the eruption signals are non-stationary over their full duration, the PSDs were estimated using a multi-taper method from isolated 10 min, 50% overlapping data segments where the assumption of stationarity is reasonable (see Figure S1). These individual spectra were then progressively averaged to form an ensemble averaged power spectrum of each signal. In the case of eruption C, the final hour of data was treated as a separate ensemble (blue lines,

<sup>1</sup>Auxiliary materials are available in the HTML. doi:10.1029/2008GL036486.

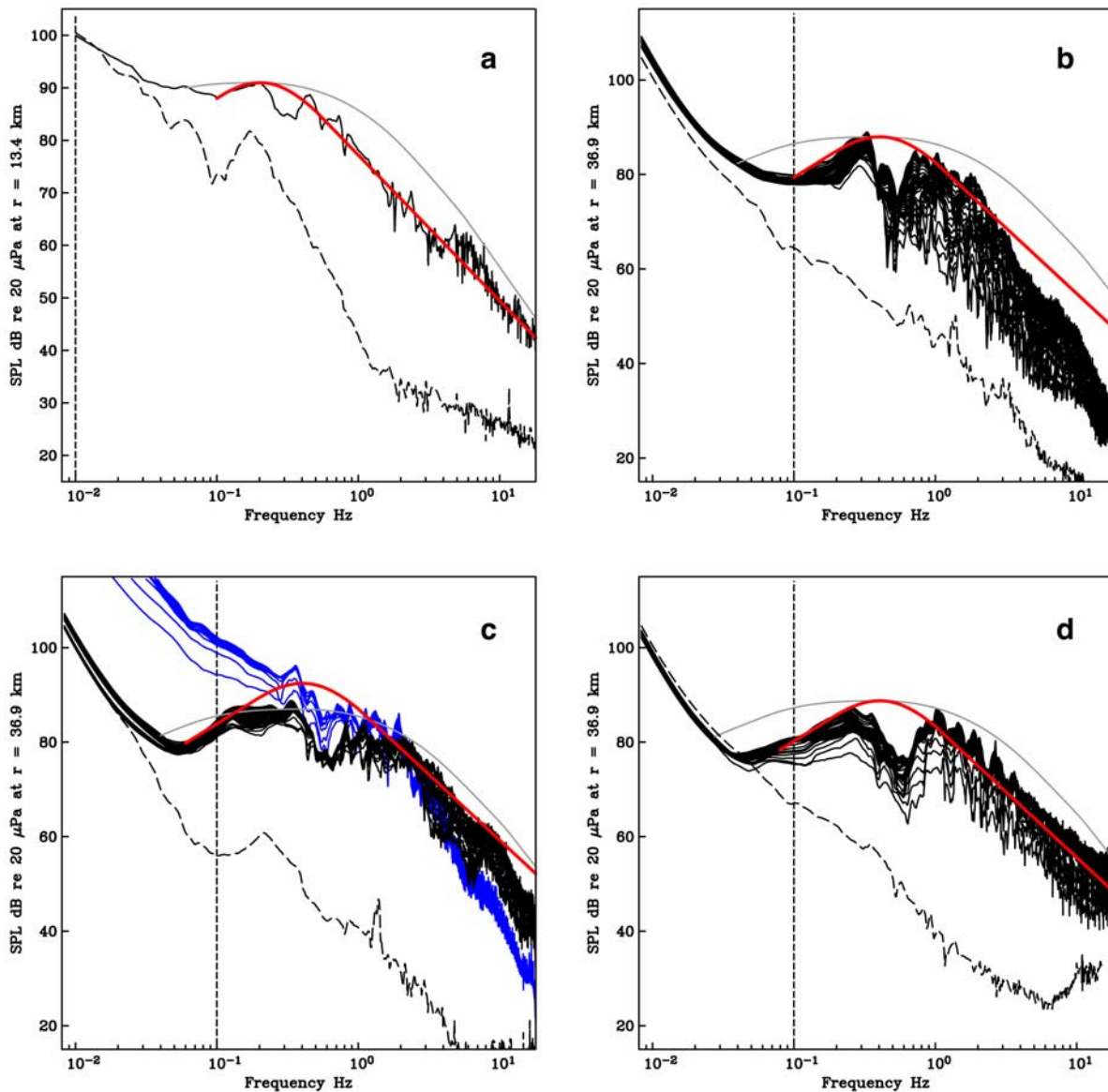


**Figure 2.** Power spectra of signals shown in Figure 1. Spectra expressed as sound pressure level (SPL) at the array in dB re  $20 \mu\text{Pa}$ . (a) 8 March 2005 MSH eruption (eruption A), (b) 14–15 July 2006 Tungurahua eruption (eruption B), (c) 16–17 August 2006 Tungurahua eruption (eruption C), (d) 6 February 2008 Tungurahua eruption (eruption D). Solid black lines represent the progressive ensemble averaged PSD of 10 min data segments (only one 6.6 min data segment in a). Dashed lines represent the background noise spectra immediately prior to or after each eruption signal (peak at  $\sim 0.2$  Hz in ambient noise for a and c is the microbarom peak). Blue lines in c represents the final hour of signal. The spectra have been corrected for instrument response. Vertical dashed lines indicate lower frequency limit of flat instrument response (3 dB point). Solid red and gray lines show the large-scale and fine-scale turbulence similarity spectra [Tam *et al.*, 1996] respectively, with peak frequency and power adjusted for comparison to data.

Figure 2). In the case of eruption A, only one 6.6 min data segment was used due to the relatively brief duration of high-amplitude eruption signal. The solid red and gray lines in Figure 2 represent the empirically-derived similarity spectra [Tam *et al.*, 1996] for large-scale and fine-scale turbulence respectively. These empirical functions represent a curve-fit to 1900 audible noise spectra measured at the NASA Langley Research Center for axisymmetric, pure-air jets sampling a wide range of Mach number and temperature [Tam *et al.*, 1996]. The overall shape and curvature of

the similarity spectra are fixed, while the two free parameters are the position of the peak frequency, and the sound pressure level (SPL) in dB. The similarity spectra should fit the entire measured spectrum. With this constraint, the best fits to the observed spectra were found for a peak frequency of 0.2 Hz for eruption A (Figure 2a), and 0.4 Hz for eruptions B–D, excluding the last hour of eruption C (Figures 2b–2d). The peak frequency for the last hour of eruption C is below the low frequency response of the

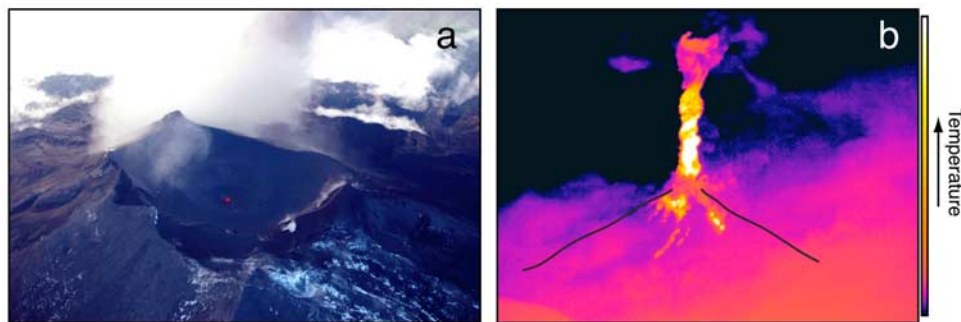


**Figure 3.** Constraints on the length-scale of Tungurahua eruption jets. (a) Aerial view of crater taken from a helicopter in February 2008,  $\sim 5$  hours before eruption D. The crater diameter is estimated at 300–400 m. (b) FLIR infrared image of 16–17 August 2006 eruption taken at 04:52:22 17 August 2006 UTC. Black lines indicate approximate mountain topography. The incandescent part of the jet reaches a height  $\sim 1.8$ – $1.9$  km above the vent. The jet-like nature of the flow is apparent. The lowermost portion of the jet is obscured by ash from pyroclastic flows descending the mountain.

sensors ( $<0.1$  Hz), but the slope of the spectrum is matched by the large-scale turbulence noise spectrum (Figure 2c).

#### 4. Discussion

[10] The peak frequencies of 0.2 Hz and 0.4 Hz are  $\sim 3$  orders of magnitude lower than those typical of the NASA data [Tam *et al.*, 1996]. However, the length-scale of the volcanic jet  $D_j$  is  $\sim 3$  orders of magnitude larger than that of the NASA data, such that the Strouhal numbers of the jet noise peak frequencies are roughly equivalent. Figure 3 shows two images that can be used to constrain the jet length-scales at Tungurahua Volcano. Figure 3a is an aerial photograph of the Tungurahua summit crater taken from a helicopter after the 2006 eruptions (eruptions B and C), just before eruption D. The diameter of the crater is  $\sim 300$ – $400$  m - an approximate measure of the jet diameter that eroded the crater. Figure 3b is a FLIR infrared image of the 16–17 August event (eruption C) taken at 17 August 04:52:22 UTC. The height of the incandescent part of the jet is estimated at  $\sim 1.8$ – $1.9$  km, and the jet diameter fills the entire summit region. Jet muzzle velocities at the vent are  $\sim 300$  m/s based on field studies of ballistics [Arellano and Hall, 2006]. Eruption A was a smaller-scale event, perhaps having a jet diameter  $\sim 30$  m, and a muzzle velocity  $\sim 100$  m/s [Mastin, 2007]. Although very approximate, these values for  $D_j$  and  $U_j$  suggest that peak frequencies of the infrasound spectra (Figure 2) correspond to  $St \sim 0.06$  for eruption A, and  $St \sim 0.4$  for eruptions B–D (excluding the final hour of eruption C). These values of  $St$  are within the observed range of  $St$  values for laboratory jets [Tam *et al.*, 1996], jet engines, and rockets. Since the jet length-scales are very large, the amplitudes of the infrasonic signals are also extremely high considering the source-receiver range (Figures 1 and 2).

[11] The large-scale turbulence (LST) similarity spectrum matches the shape of the infrasonic spectra reasonably well (red lines, Figure 2), while the fine-scale turbulence (FST) similarity spectrum [Tam *et al.*, 1996] (gray lines, Figure 2) does not match as well. In laboratory studies, LST noise is usually dominant in a narrow beam surrounding the downstream direction of the jet, while FST noise is dominant at  $\sim 90^\circ$  from the jet axis - the relevant angle for far-field ground observations of a vertical volcanic jet. However, the low frequencies considered may lead to strong diffraction

effects, such that source directionality may be less prominent. Furthermore, as jet temperature increases, LST noise is dominant over a wider angular sector for hot jets [Tam *et al.*, 1996]. Core temperatures are high for a volcanic jet, and higher for the magmatic eruptions B–D than for the phreatic eruption A.

[12] The LST similarity spectrum matches the shape of the spectrum for the full range of frequencies for eruption A (Figure 2a), but has discrepancies for eruptions B–D (Figures 2b–2d). The spectra for B–D have a significant notch of diminished amplitudes centred at  $\sim 0.4$ – $0.6$  Hz, and the roll-off at high frequencies ( $>3$  Hz) is not well matched for B and C. These features could be explained by complexities of the volcanic source not found in pure-air laboratory jets. The phreatic eruption A had a different fluid composition and quantity of solid particle-loading than the magmatic eruptions B–D. Although the pseudogas approximation is often used to model volcanic jets [Kieffer and Sturtevant, 1984], two-phase jet flows are known to be different to pure-air jet flows. For instance, particle image velocimetry (PIV) measurements have shown that turbulent Reynolds stresses are modified by the presence of heavy particles [Seiner *et al.*, 2003]. Drag force on particles can lower the flow velocity of a mixture [Chojnicki *et al.*, 2006], which may result in a lower frequency of acoustic radiation. It is also possible that large particles travel with a separate, slower velocity to the gas phase, which may explain the double-peaked nature of the spectra for B–D. In addition, since the particles are incompressible, they may generate boundary layer noise in the turbulent flow [Woulff and McGetchin, 1976]. Turbulent interaction with solid particles or crater walls may generate one frequency peak, while the other is generated by LST noise within the jet. The difference between the magmatic eruptions B–D and the phreatic eruption A may also be attributable to temperature effects. We note that the notch at  $\sim 0.4$ – $0.6$  Hz for B–D was observed at an identical array  $\sim 250$  km north of Tungurahua, suggesting that this is a source feature rather than a propagation effect such as ground-bounce interference.

#### 5. Conclusions

[13] Despite the complexities discussed above, the overall features of the infrasonic signals accompanying volcanic eruptions are remarkably similar to those of jet noise. In

addition, the fact that eruptions A and D have spectra following the overall shape of the LST similarity spectrum suggests that, despite a length-scale difference of  $\sim 3$  orders of magnitude, the fundamental noise-generation mechanisms occurring in volcanic jets are similar to those occurring in man-made jets. However, the additional complexities in the volcanic signals point to directions of future research necessary for a better understanding of volcanic jet noise. Laboratory aeroacoustic studies are required to study the effects of heavy particulate loading, very high temperatures, and complex crater morphology on radiated jet noise spectra and acoustic power. A long-term goal of these studies would be to estimate volcanic jet parameters such as the expanded jet diameter and velocity, volume flux, fluid composition, and vent overpressure from broadband acoustic recordings. These parameters are essential for a quantitative understanding of explosive volcanic eruption dynamics, and would aid substantially in ash dispersal modelling and the remote assessment of volcanic hazard.

[14] **Acknowledgments.** We thank Bernard Chouet, Kent Gee, and Larry Mastin for thoughtful suggestions, and Maurizio Ripepe for a critical review. The infrasound data were collected by the Acoustic Surveillance for Hazardous Eruptions (ASHE) program. We used a multitaper PSD code written by Bob Parker. This work was funded by NSF grant EAR-0609669. We dedicate this paper to the memory of our friend and mentor Henry E. Bass, who was fascinated by this research and would have been a co-author.

## References

- Arellano, S., and M. Hall (2006), Velocidades de emisión de bombas expulsadas por el Volcán Tungurahua el 16–17 de Agosto de 2006, paper presented at 6th Jornadas en Ciencias de la Tierra, Dep. de Geol. y Riesgos, Nat. de la Escuela Politéc. Nac., Quito, Ecuador.
- Barba, D., S. Arellano, P. Ramón, P. Mothes, A. Alvarado, G. Ruiz, and L. Troncoso (2006), Cronología de los Eventos Eruptivos de Julio y Agosto del 2006 del Volcan Tungurahua, paper presented at 6th Jornadas en Ciencias de la Tierra, Dep. de Geol. y Riesgos, Nat. de la Escuela Politéc. Nac., Quito, Ecuador.
- Chojnicki, K., A. B. Clarke, and J. C. Phillips (2006), A shock-tube investigation of the dynamics of gas-particle mixtures: Implications for explosive volcanic eruptions, *Geophys. Res. Lett.*, *33*, L15309, doi:10.1029/2006GL026414.
- Chouet, B. A. (1996), New methods and future trends in seismological volcano monitoring, in *Volcanic Seismology: IAVCEI Proceedings in Volcanology*, vol. 3, edited by R. Scarpa and R. Tilling, pp. 23–97, Springer, Berlin.
- Crow, S. C., and F. H. Champagne (1971), Orderly structure in jet turbulence, *J. Fluid Mech.*, *48*, 547–591.
- Garcés, M., et al. (2008), Capturing the Acoustic Fingerprint of Stratospheric Ash Injection, *Eos Trans. AGU*, *89*(40), doi:10.1029/2008EO400001.
- Garcés, M. A., M. T. Hagerty, and S. Y. Schwartz (1998), Magma acoustics and time-varying melt properties at Arenal Volcano, Costa Rica, *Geophys. Res. Lett.*, *25*, 2293–2296.
- Johnson, J. B., M. C. Ruiz, J. M. Lees, and P. Ramon (2005), Poor scaling between elastic energy release and eruption intensity at Tungurahua Volcano, Ecuador, *Geophys. Res. Lett.*, *32*, L15304, doi:10.1029/2005GL022847.
- Kieffer, S. W., and B. Sturtevant (1984), Laboratory studies of volcanic jets, *J. Geophys. Res.*, *89*, 8253–8268.
- Lighthill, M. J. (1954), On sound generated aerodynamically II. Turbulence as a source of sound, *Proc. R. Soc. London, Ser. A*, *222*, 1–32.
- Lilley, G. M. (1991), Jet noise classical theory and experiments, in *Aeroacoustics of Flight Vehicles: Theory and Practice*, vol. 1, edited by H. H. Hubbard, Acoust. Soc. of Am., Melville, N. Y.
- Mastin, L. G. (2007), A user-friendly one-dimensional model for wet volcanic plumes, *Geochem. Geophys. Geosyst.*, *8*, Q03014, doi:10.1029/2006GC001455.
- Matoza, R. S., M. A. H. Hedlin, and M. A. Garcés (2007), An infrasound array study of Mount St. Helens, *J. Volcanol. Geotherm. Res.*, *160*, 249–262.
- McNutt, S. R. (2000), Seismic monitoring, in *Encyclopedia of Volcanoes*, edited by H. Sigurdsson, Academic, San Diego, Calif.
- Ogden, D. E., K. H. Wohletz, G. A. Glatzmaier, and E. E. Brodsky (2008), Numerical simulations of volcanic jets: Importance of vent overpressure, *J. Geophys. Res.*, *113*, B02204, doi:10.1029/2007JB005133.
- Pope, S. B. (2005), *Turbulent Flows*, Cambridge Univ. Press, New York.
- Ripepe, M., P. Poggi, T. Braun, and E. Gordeev (1996), Infrasonic waves and volcanic tremor at Stromboli, *Geophys. Res. Lett.*, *63*, 181–184.
- Seiner, J. M. (1984), Advances in high speed jet aeroacoustics, *AIAA Pap.* 84-2275.
- Seiner, J. M., L. G. Gui, L. Ukeiley, and B. J. Jansen (2003), Particle laden jet PIV Experiments and simulations, paper presented at 9th Spirits JAN-NAF Meeting, Joint Army Navy NASA Air Force Interagency Propul. Comm., Bay St. Louis, Miss.
- Tam, C. K. W. (1995), Supersonic jet noise, *Annu. Rev. Fluid Mech.*, *27*, 17–43.
- Tam, C. K. W. (1998), Jet noise: Since 1952, *Theor. Comput. Fluid Dyn.*, *10*, 393–405.
- Tam, C. K. W., M. Golebiowski, and J. M. Seiner (1996), On the two components of turbulent mixing noise from supersonic jets, *AIAA Pap.* 96-1716.
- Vergnolle, S., and J. Caplan-Auerbach (2006), Basaltic thermals and Subplinian plumes: Constraints from acoustic measurements at Shishaldin Volcano, Alaska, *Bull. Volcanol.*, *68*, 611–630.
- Wilson, C. R., and R. B. Forbes (1966), Infrasonic waves from Alaskan volcanic eruptions, *J. Geophys. Res.*, *74*, 4511–4522.
- Wilson, L. (1976), Explosive volcanic eruptions-III. Plinian eruption columns, *Geophys. J. R. Astron. Soc.*, *45*, 543–556.
- Woulff, G., and T. R. McGetchin (1976), Acoustic noise from volcanoes: Theory and experiment, *Geophys. J. R. Astron. Soc.*, *45*, 601–616.
- D. Fee and M. A. Garcés, Infrasound Laboratory, University of Hawai'i, 73-4460 Queen Kaahumanu Highway 119, Kailua-Kona, HI 96740, USA. (dfee@isla.hawaii.edu; milton@isla.hawaii.edu)
- M. A. H. Hedlin and R. S. Matoza, Institute of Geophysics and Planetary Physics, IGPP 0225, Scripps Institution of Oceanography, University of California, San Diego, La Jolla, CA 92093-0225, USA. (hedlin@ucsd.edu; rmatoza@ucsd.edu)
- P. A. Ramón, Instituto Geofísico, Escuela Politécnica Nacional, P.O. Box 2759, Quito, Ecuador. (pramon@igepn.edu.ec)
- J. M. Seiner, National Center for Physical Acoustics, University of Mississippi, 1 Coliseum Drive, University, MS 38677, USA. (jseiner@olemiss.edu)